Effect of magnetic fine structure and mixing on the radiative lifetimes and the polarizabilities of excited states of helium

W. G. Schoenfeld and E. S. Chang
Department of Physics and Astronomy, University of Massachusetts, Amherst, Massachusetts 01003
(Received 3 November 1993)

We have calculated the radiative lifetimes, and the scalar and tensor dipole polarizabilities of excited levels of helium. Our theory includes fine structure and the mixing of singlet and triplet sublevels, and gives results that are in excellent agreement with experiment. We are able to show why fine structure and mixing have negligible effects on the radiative lifetimes, but may contribute up to 20% of the polarizabilities. The trends of these properties with the quantum numbers n and L are explicated, and formulas are given which are accurate to a few percent for arbitrary n and $L \geq 2$.

PACS number(s): 32.60.+i, 32.70.Jz, 35.10.Di

I. INTRODUCTION

The radiative lifetimes and the dipole polarizabilities of excited levels depend on the same set of matrix elements and transition energies. Recently, accurate values for these matrix elements in helium have become available through the laborious correlated wave function calculations of Kono and Hattori [1,2]. Shortly afterwards, we had investigated the fine-structure energy levels and the problem of singlet-triplet mixing in helium [3]. The time has come for a careful calculation of the lifetimes and polarizabilities, which includes both the most accurate matrix elements, and a proper accounting of fine structure and mixing effects. The present work reports on these results and compares them with those from earlier theories and experiments.

A comprehensive calculation of radiative lifetimes τ has been carried out in helium for Rydberg levels up to principal quantum number n=20 and orbital quantum number L=3. In that work [4], Theodosiou employed a model potential and ignored the magnetic fine structure and the mixing of singlet and triplet levels. We have calculated the lifetimes of each magnetic sublevel, and demonstrated that for each set of triplet sublevels, their values are well within 0.1% of each other. It turns out that our elaborate results seldom differ from Theododiou's by more than one percent. We will explain why, the inclusion of magnetic fine structure and mixing does not significantly alter the lifetimes. We will show that τ varies in a predictable way in L as well as in n, contrary to a statement by Theodosiou. In fact for $L \geq 3$, the lifetimes are hydrogenic to an accuracy of a few percent. Thus, they can be evaluated by a simple formula [5,6], and so extensive compilations [7] are largely unnecessary.

The tensor polarizability $\alpha_{\rm ten}$ of excited levels in helium as well as some lifetimes have been extensively studied by von Oppen and co-workers [8–11] and others [12,13]. To facilitate comparison with their measurements, they used a theory based upon simple Coulomb matrix elements in the LS-coupling approximation. We will show that although the matrix elements important for the lifetimes may differ by more than 10% from the corresponding hydrogenic values, the ones important in determining $\alpha_{\rm ten}$ differ by less than 1%. For the D levels, we will explicitly show that mixing is unimportant. Therefore, their simple theoretical results [8,10] are accurate to almost 1%. Moreover, the values of $\alpha_{\rm ten}$ for the three triplet sublevels are accurately related by the ratios obtained in LS coupling [14]. In contrast, Aynacioglu *et al.* [11] demonstrated that for the $4f\ ^1F_3$ sublevel, the Coulomb value differs from their measured one by 25%. Using an *ad hoc* theory, they were able to attribute most of the discrepancy to mixing. In this work, we derive from first principles, an expression for the tensor polarizabilities of the singlet sublevels which explicitly takes into account the singlet-triplet mixing. Similar to, but not the same as theirs, our expression explains why mixing is important for the $4f\ ^1F_3$ but not for the $5f\ ^1F_3$ sublevel. In addition to the tensor, we also calculate the scalar polarizabilities $\alpha_{\rm sc}$. For circular states, we show that $\alpha_{\rm sc} \simeq -\alpha_{\rm ten}$. However for noncircular states, they are approximately related by other ratios. Finally, we discuss the n and L dependence of both polarizabilities, and give formulas accurate to a few percent for higher values of n and L.

II. THEORY

The radiative lifetime and the dipole polarizabilities of atomic excited states share the trait that they depend on the same dipole matrix elements and energy differences. Usually the dipole matrix elements and energies are calculated in the LS-coupling scheme. In this work, we explore the consequences of the magnetic interactions that cause the fine-structure splitting of the energy levels and the mixing of certain wave functions. The theory which accounts for mixing has been explicitly given for helium in the context of fine-structure line intensities [3]. Following that work, it is straightforward to derive the

following expressions for the lifetimes and the polarizabilities.

A. Radiative lifetime

The radiative lifetime of atomic excited states has been reviewed by Verolainen and Nikolaich [15]. By definition it is given by

$$\tau_u = \frac{1}{\sum_l A(u \to l)}, \tag{1}$$

where u and l stand for the upper and the lower level, each characterized by a set of quantum numbers, $\{n, L, S, J\}$. The Einstein A coefficient from $u = \{n, L, S, J\}$ to $l = \{n', L', S', J'\}$ is defined as

$$A(u \to l) = 4\alpha^3\sigma^2 \frac{2J'+1}{2J+1} f(l \to u), \tag{2}$$

where α is the fine-structure constant, and the absorption oscillator strength is given by

$$f(l \to u) = \frac{\sigma}{3(2J'+1)} |\langle nLSJ \parallel \mathbf{r} \parallel n'L'S'J' \rangle|^2. \tag{3}$$

The transition frequency is given by $\sigma = (E_{nLSJ} - E_{n'L'S'J'})/(hc)$, where E_{nLSJ} stands for the energy of the sublevel, and h and c are Planck's constant and the velocity of light. The usual selection rules dictate that A_{ul} vanishes unless $L' = L, L \pm 1$, $J' = J, J \pm 1$, and $S' = S$. The bound states of helium are described by the configuration $1sn\ell$, so $L = \ell$, thus Laport's Rule excludes transitions in which $L = L'$. As discussed later in Sec. II C on singlet-triplet mixing, S' may now take on the values 0 or 1. Note that factors of σ in the numerator of $A(u \to l)$ accentuates the contribution from the lowest levels permitted by the selection rules. On the other hand, contributions from the highest levels (with $n' = n$) almost vanish especially when L is sufficiently large. Consequently, states which are dipolarly connected to the ground level can be expected to have exceptionally short lifetimes, such as the $1snp\ ^1P$ levels of helium.

B. Dipole polarizabilities

In an electric field of strength $\mathcal{E}$ with z component $\mathcal{E}_z$, the energy shift due to the quadratic Stark effect [14] is given by

$$\Delta E = -\frac{1}{2}\alpha_S \mathcal{E}^2 - \frac{1}{4}\alpha_T \frac{3M^2 - J(J+1)}{J(2J+1)} (3\mathcal{E}_z^2 - \mathcal{E}^2). \tag{4}$$

The scalar and tensor polarizabilities of the state $\{nLSJ\}$ are defined as follows:

$$\alpha_S = -\frac{2e^2}{3(2J+1)} \sum_{n',L',S',J'} \frac{|\langle nLSJ \| \mathbf{r} \| n'L'S'J' \rangle|^2}{E_{nLSJ} - E_{n'L'S'J'}}, \tag{5}$$

and

$$\alpha_T = -4e^2 \left(\frac{5J(2J-1)}{6(2J+3)(J+1)(2J+1)} \right)^{1/2} \times \sum_{n',L',S',J'} (-1)^{J'+J} \begin{Bmatrix} 1 & 1 & 2 \\ J & J & J' \end{Bmatrix} \times \frac{|\langle nLSJ \| \mathbf{r} \| n'L'S'J' \rangle|^2}{E_{nLSJ} - E_{n'L'S'J'}}, \tag{6}$$

where the braces stand for the Racah $6j$ symbol. In contrast to the expression for the lifetime which varies as σ^3, here σ appears in the denominator rather than in the numerator. Hence the polarizabilities are dominated by the resonance terms with $n' = n$.

C. Matrix elements in the mixed representation

Going beyond the LS representation, states in the mixed representation are superpositions of wave functions with the same values of L and J. We now focus on the two-electron system pertinent to helium. In the mixed representation, the wave functions are designated by $\{nLSJ\}$ and are simply described as

$$|\, nLSJ\rangle = \psi_{nL0}\{\beta\} + \psi_{nL1}\{\gamma\}, \tag{7}$$

where ψ_{nL0} and ψ_{nL1} are the singlet and the triplet wave functions, respectively in the LS representation. The ith singlet β_i and triplet γ_i component amplitudes for the four sublevels $\{L0L,\ L1L,\ L1L-1,\ L1L+1\}$ are $\{\beta\} = \{\cos\theta_{nL}, -\sin\theta_{nL}, 0, 0\}$ and $\{\gamma\} = \{\sin\theta_{nL}, \cos\theta_{nL}, 1, 1\}$. The mixing angle θ_{nL} for helium is found [3] to depend only weakly on n as depicted in Fig. 1. Typical values are $0.02°, 0.5°, 30°$, and $44°$ for L=1, 2, 3, and 4, respectively, which imply negligible mixing for $L \leq 2$, but strong mixing for $L \geq 3$. The squared reduced matrix element for initial and final states ni and $n'i'$ can then be evaluated as

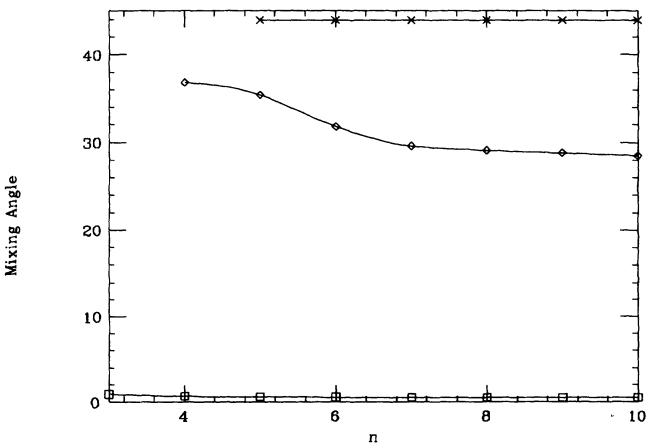

FIG. 1. Mixing angles θ in degrees for helium D (squares), F (diamonds), and G (crosses) levels.

$$|\langle ni\|\mathbf{r}\|n'i'\rangle|^2 = |\langle nLSJ\|\mathbf{r}\|n'L'S'J'\rangle|^2$$
$$= L_>(2J+1)(2J'+1)$$
$$\times\left[\frac{\beta_i\beta_{i'}R_{nL}^{n'L'}(0)}{[(2L+1)(2L'+1)]^{1/2}}\right.$$
$$\left.-\gamma_i\gamma_{i'}R_{nL}^{n'L'}(1)\begin{Bmatrix} L & J & 1 \\ J' & L' & 1 \end{Bmatrix}\right]^2. \quad (8)$$

As usual $L_>$ stands for the greater of (L, L'), and $R_{nL}^{n'L'}(0)$ and $R_{nL}^{n'L'}(1)$ stand for the relevant radial dipole matrix elements for the singlet and triplet system, respectively. For the present computations, the fine-structure energy levels are taken from Chang [3] and Martin [16], while the radial matrix elements for P-D transitions are extracted from the f values of Kono and Hattori [1], those for D-F transitions come from Theodosiou [7]. For $L \geq 3$, the matrix elements are assumed to be hydrogenic and are calculated from expressions given by Bessis *et al.* [17]. We have also examined the contribution of the induced dipole moment to the electric dipole operator [18], and found that the correction is negligible, being typically only 0.01%.

III. RADIATIVE LIFETIMES FOR HELIUM

A. Results and discussions

The radiative lifetimes of helium have been calculated by Theodosiou [4] in the Hartree-Slater approximation for $L = 0, 1, 2$, and 3 and for $n \leq 20$. He has shown that his f values agree with those from more accurate calculations in the LS representation to about 1%. In Fig. 2, we compare his values for the dipole matrix elements, $R_{2p}^{nd}(0)$ and $R_{2p}^{nd}(1)$ with those from a recent thousand-term variational calculation by Kono and Hattori [1]. Expressed as ratios to the corresponding hydrogenic matrix elements, the two sets are seen to agree well within a fraction of 1%. The singlet ratios decrease from above to below unity as n increases, while the triplet ratios behave in exactly the opposite manner, with the two curves crossing around n=5. Ratios for related matrix elements where $2p$ is replaced by $n'p$ $(n' < n)$ exhibit the same trend. For S states there is no mixing; for P states mixing is negligibly small, also the fine-structure splitting is small compared with the nS-$n'P$ and the nP-$n'S$ spacing. Therefore Theodosiou's neglect of these effects is well justified. However, for levels with $L \geq 3$ mixing angles can be quite large, and it is, in principle, possible for the lifetimes of the three triplet sublevels to be quite different from each other as well as from the value in the LS representation.

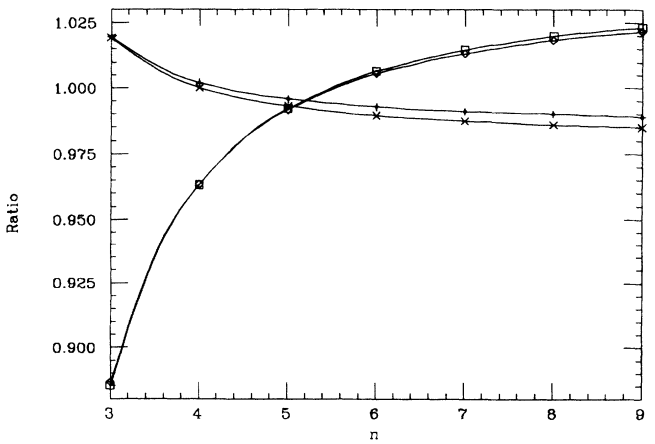

FIG. 2. Ratios of the radial matrix elements $\langle 2p|r|nd\rangle$ for helium to hydrogen. Singlet results are given by KH (crosses) and by Theodosiou (bars), while the triplet results are given by KH (diamonds) and by Theodosiou (squares).

Using the method described in Sec. II, we calculate the radiative lifetimes of the nd, nf, and ng levels in helium. Some results are shown in Table I along with the results of Theodosiou and recent measurements. Disappointingly, our calculated values for the triplet sublevels generally differ from each other by only 0.01%. Further, our results including fine structure and mixing are virtually identical to those of Theodosiou who neglected them; both are in good agreement with experiment. For greater consistency, when possible we choose to display the results of von Oppen and collaborators who also measure tensor polarizabilities (Sec. IV). The minute difference between the two theories is typically an order of magnitude less than the experimental uncertainty. To understand why these effects do not affect the lifetime significantly, we list the individual contributing Einstein A coefficients for some lifetimes in Table II. For the $3d\ ^1D_2$ sublevel, the lifetime is dominated by the transition to the $2p\ ^1P_1$ sublevel, since the other A coefficients are at least three orders of magnitudes smaller. Similarly the $3d\ ^3D_3$ lifetime is dominated by the transition to the $2p\ ^3P_2$ sublevel. However, for the $3d\ ^3D_2$ sublevel, two A coefficients are large: the ones to the $2p\ ^3P_1$ and $2p\ ^3P_2$ sublevels. Nevertheless their sum is essentially the same as the dominant A coefficient of the $3d\ ^3D_3$ sublevel, so the lifetimes of the two sublevels $3d\ ^3D_2$ and $3d\ ^3D_3$ are nearly the same. In fact, the above approximate equality becomes exact if we neglect the fine-structure splittings

TABLE I. Helium radiative lifetimes (nanoseconds).

Level	Present work	Theodosiou[a]	Experiment	Eq. (10)
$1s3d\ ^1D$	15.70	15.69	15.3 (3.0)[b]	15.7
$1s3d\ ^3D$	14.14	14.18	14.25 (0.34)[c]	15.7
$1s4d\ ^1D$	37.08	36.96	38.7 (2.4)[b]	37.3
$1s4d\ ^3D$	32.50	32.07	32.1 (1.3)[c]	37.3
$1s5d\ ^1D$	71.84	71.52	70 (5)[b]	72.8
$1s5d\ ^3D$	60.94	60.89	57.2 (2.3)[c]	72.8
$1s4f\ ^1F$	72.34	72.31	74 (2)[d]	73.1
$1s5f\ ^1F$	139.8	139.7	133 (5)[d]	142.7
$1s5g\ ^1G$	234.8		230 (20)[e]	235.9

[a]Reference [4].
[b]Reference [9].
[c]Reference [10].
[d]Reference [11].
[e]Reference [19].

of both sublevels when compared with the $2p$-$3d$ spacing. This can be proven analytically by a well-known sum rule of the $6j$ symbols. Similarly for the $3d\ ^3D_1$ sublevel, the three largest A coefficients sum up very closely to the dominant A coefficient of the $3d\ ^3D_3$ sublevel, so it also has essentially the same lifetime. Thus, the three triplet lifetimes are all very close to the Hartree-Slater value because the mixing angles are small, and the fine-structure splittings are negligibly small as compared with the $2p\ ^3P$–$3d\ ^3D$ spacing.

Beginning with the $5d$ level, transitions to the $n'f$ levels also contribute to the lifetime. However, Table II shows that these A coefficients are typically two orders of magnitude less than those to the $n'p$ levels. So the large mixing angle for F levels cannot be expected to affect the lifetime significantly. Therefore, the previous discussion of the $3d$ levels also applies to the $5d$ or any nd levels. Actually we have calculated the Einstein A coefficients for all fine structure sublevels to all other sublevels allowed by the selection rules for $n \leq 10$, but have tabulated only a very limited subset in Table II as samples.

We recall that F levels have large mixing angles of about 30°, so their lifetimes can be expected to deviate significantly from the Hartree-Slater values. However, comparison of our results with those of Theodosiou in Table I show that this is not the case. As expected, mixing causes the $4f\ ^1F_3$ level to have sizeable A coefficients for the "forbidden" transitions to the $3d\ ^3D_2$ and $^3D_3$ sublevels, while decreasing the A coefficient to the "allowed" $3d\ ^1D_2$ sublevel. However, their sum is virtually the same as the single A coefficient for the only "allowed" $4f\ ^3F_4$–$3d\ ^3D_3$ transition. Once again, whenever the fine-structure splittings are negligible compared with the $3d$-$4f$ spacing, the $6j$ symbol sum rule prevails. Further, the singlet and the triplet radial matrix elements are nearly equal; both are within half a percent of the hydrogenic value [17]. Similar results are obtained for the $4f\ ^3F_3$ and the $4f\ ^3F_2$ sublevels. Therefore, all $4f$ sublevels have virtually identical lifetimes, requiring only one value to be listed in Table I. From the above discussion, it is evident that lifetimes will be significantly different in the mixed and the L-S representations only when the mixing angle and the fine-structure splittings are large simultaneously. The above condition does not exist in helium since the low L levels have large splittings but small mixing angles, while the high L levels have large mixing angles but

TABLE II. Calculated radiative lifetimes τ(nsec) and Einstein A coefficients ($\sec^{-1}$).

Initial state	$3d\ ^1D_2$, τ=15.704	$3d\ ^3D_1$, τ=14.142	$3d\ ^3D_2$, τ=14.143	$3d\ ^3D_3$, τ=14.144
Final state	A coeff.	A coeff.	A coeff.	A coeff.
$2p\ ^1P_1$	6.366×10^7	2.237	1.503×10^4	
$2p\ ^3P_0$		3.927×10^7		
$2p\ ^3P_1$	1.222×10^4	2.946×10^7	5.301×10^7	
$2p\ ^3P_2$	4.314×10^3	1.964×10^6	1.767×10^7	7.069×10^7
$3p\ ^3P_0$		7.182×10^3		
$3p\ ^3P_1$	2.312	5.395×10^3	9.707×10^3	
$3p\ ^3P_2$	0.805	3.597×10^2	3.236×10^3	1.295×10^4

Initial state	$5d\ ^1D_2$, τ=71.835	$5d\ ^3D_1$, τ=60.945	$5d\ ^3D_2$, τ=60.942	$5d\ ^3D_3$, τ=60.941
Final state	A coeff.	A coeff.	A coeff.	A coeff.
$2p\ ^1P_1$	8.984×10^6	0.416	8.761×10^2	
$2p\ ^3P_0$		6.443×10^6		
$2p\ ^3P_1$	8.319×10^2	4.832×10^6	8.698×10^6	
$2p\ ^3P_2$	2.996×10^2	3.221×10^5	2.899×10^6	1.159×10^7
$3p\ ^1P_1$	3.359×10^6	0.097	3.316×10^2	
$3p\ ^3P_0$		1.932×10^6		
$3p\ ^3P_1$	2.502×10^2	1.449×10^6	2.609×10^6	
$3p\ ^3P_2$	8.988×10^1	9.663×10^4	8.695×10^5	3.478×10^6
$4p\ ^1P_1$	1.525×10^6	0.030	1.516×10^2	
$4p\ ^3P_0$		7.114×10^5		
$4p\ ^3P_1$	9.148×10^1	5.336×10^5	9.605×10^5	
$4p\ ^3P_2$	3.312×10^1	3.557×10^4	3.201×10^5	1.280×10^6
$5p\ ^3P_0$		8.438×10^2		
$5p\ ^3P_1$	0.114	6.338×10^2	1.140×10^3	
$5p\ ^3P_2$	0.040	4.226×10^1	3.802×10^2	1.521×10^3
$4f\ ^1F_3$	3.251×10^4		1.576×10^4	1.449×10^3
$4f\ ^3F_2$	0.578	5.026×10^4	5.584×10^3	1.140×10^2
$4f\ ^3F_3$	1.781×10^4		2.891×10^4	2.540×10^3
$4f\ ^3F_4$				4.616×10^4

small splittings.

For G and higher L levels, the mixing angles are all near the maximum value of 45° (see Fig. 1). Nevertheless our calculations reveal that the lifetimes of the four sublevels for a given level nL always agree with each other to within 0.001%. For example, the lifetimes of all four $5g$ sublevels are identical to five significant places, and are clearly all consistent with the measured $^1G_4$ value [19] given in Table I. It can be easily verified that for a given $5g$ sublevel, the sum of the A coefficients to all $4f$ sublevels is invariant, and matches the A coefficient for the $5g\ ^3G_5$–$4f\ ^3F_4$ transition. This result follows from the fact that the fine-structure splitting becomes completely negligible when compared with the Rydberg level spacing, and so the sum rule may again be applied. Since the radial matrix elements for higher L are even closer to the hydrogenic values, we find that the lifetimes for G and higher L levels are hydrogenic to well within 0.1%. Some of these hydrogen lifetimes are listed in Table I of the review Ref. [15].

B. Analytic fits and trends in lifetimes

For the purpose of extrapolation, Theodosiou has fitted his calculated lifetimes from n=15 to 20 to the power law:

$$\tau = \tau_0 (n^*)^\gamma, \tag{9}$$

where n^* is the effective quantum number. His values for γ are all nearly 3 (within one or two percent) for L from 0 up to 3, for both $S = 0$ and 1. We have fitted our entire series for $L \geq 2$, from the lowest value of n up to n=10 substituting n for n^* in Eq. (9). Actually, we have tried both n and n^*, and found that the difference is considerably less than 1%. Therefore, we opt for using n since it is easier to apply and allows for a direct comparison of the singlet and the triplet cases. Table III displays the fitted coefficients with the statistical errors. A comparison of the lifetimes calculated with Eq. (9) and the parameters from Table III shows that they agree to within 1% with our elaborate ones, or Theodosiou's. Thus, they appear to be sufficiently accurate for comparison with most experiments. (See experimental errors in Table I.)

From Table III, it is evident that the ^1D series has a longer lifetime than the corresponding ^3D series, since both γ and τ_0 are larger for the singlet case. The main reason is that the singlet transition energies are about 10% smaller than the triplet ones, which more than makes up for the fact that the singlet matrix element is larger than the triplet for low values of n as depicted in Fig. 2. On the other hand, the ^1F and ^3F levels have the same lifetimes (as is the case with higher L levels) because the singlet-triplet splitting (the exchange energy) becomes negligibly small as L increases. Table III shows that τ_0 for the F series is about twice that of the D series . Unfortunately, Theodosiou made an error in fitting his ^1F series, resulting in too small a value for τ_0 by a factor of about 20. Consequently the error in his figures for the lifetimes led him to conclude that their ordering in magnitude did not follow the value of L.

TABLE III. Power-law-fitting coefficients for τ(nsec).

Series	γ	Error	τ_0	Error
^3D	2.8895	0.0083	0.5886	0.0080
^1D	2.9650	0.0024	0.6064	0.0024
F	2.9944	0.0010	1.2207	0.0010
G	2.9452	0.0017	2.0561	0.0013

In contrast, we find that the lifetime pattern is well ordered in L, according to the hydrogenic upper bound value [5]

$$\tau \leq \tau_u (L + 1/2)^2 n^3 \quad (L > 0)\ , \tag{10}$$

where τ_u=93.4 ns. It has been shown [5], that the upper bound values given by Eq. (10) seldom exceeds the calculated hydrogenic lifetimes [15] by 10%. In addition, Eq. (10) has also been derived semiclassically with an estimate of its error [6]. In fact, the last column of Table I shows how well Eq. (10) agrees with the helium lifetimes. In the case of the helium ^1D lifetimes, the agreement is coincidental. Figure 2 reveals that the singlet radial matrix elements in helium are within 2% of the hydrogenic values. Similarly, the singlet transition energies are about 2% smaller than the hydrogenic values. Hence the ^1D lifetimes are nearly hydrogenic. However for the ^3D case, the frequencies are about 10% larger than the hydrogenic values, leading to larger A coefficients and hence shorter lifetimes. Beginning with the F levels, the helium matrix elements and transition frequencies are always well within 1% of the corresponding hydrogenic value. Therefore their lifetimes are hydrogenic for all practical purposes, and may be represented by Eq. (10) to almost the experimental accuracy of 5–10 %. Thus, the trend in L of the helium lifetimes for the same n is clear: $\tau \propto (L+1/2)^2$ for $L \geq 2$, and independent of S, with the mild exception of the ^3D case noted above. For example, the nf to nd lifetime ratio is $(3.5/2.5)^2$=1.96, and from Table I we see that this value is indeed about 2.

We emphasize that Eq. (10) should never be applied to S levels (even for hydrogen), since its derivation is based on the assumption that the transitions $nL \rightarrow n'L - 1$ dominate, when they actually vanish for S levels. In fact Verolainen and Nikolaich [15] have shown that the power law Eq. (9) fails for S levels, a fit requires γ to vary from 1.42 to 2.81 for different ranges of n values. Similarly for helium, for both the ^1S and the ^3S levels, log-log plots of the lifetimes versus n^* show considerable curvature [4]. Indeed, both helium lifetimes are shorter than the corresponding hydrogenic ones because the larger helium matrix elements more than make up for departures in the transition energies from hydrogen. Nor does Eq. (10) apply to P levels in helium. Like the S levels, the ^3P levels are metastable in that they cannot decay to the ground state. Therefore their lifetimes are much longer than those for the P levels in hydrogen which are not metastable. On the other hand, the ^1P levels in helium are not metastable and have much larger transition frequencies than the corresponding P levels in hydrogen. In fact the helium transition energies, in excess of 20 eV, are the highest in any atom. Therefore the helium ^1P lifetimes are the shortest of all series and among all atoms.

IV. SCALAR AND TENSOR POLARIZABILITIES

We recall that in the expressions for the scalar and the tensorial polarizabilities, Eqs. (5) and (6), the transition energies occur in the denominator. Since the resonance energies where $n' = n$ are typically two orders of magnitude smaller than the nonresonant ones ($n' \neq n$), the resonance terms totally dominate the sum. Using the method described in Sec. II, we have calculated the tensor polarizabilities of helium excited states for which experimental measurements are available. Displayed in Table IV are our results in three stages of approximation: No mix, where only the $n' = n$ terms are included and the mixing angles are set to zero; one mix, where again only the $n' = n$ terms are included but with mixing; and all mix, which includes mixing and all significant n' terms. For ease in comparison with experiment we have converted from atomic units to kHz/(V/cm)^2 [$1a_0^3 = 2.4886 \times 10^{-7}$ kHz/(V/cm)^2]. For most of the levels, the three approximation stages yield results which are virtually indistinguishable from each other, and all are in excellent agreement with experiment. This suggests that neither mixing nor contributions from nonresonance terms are important. One mild exception is the $3d\ ^3D_3$ level, where the contribution from terms where $n' \neq n$ is about 4%. Experiment clearly favors the all mix result which is the most complete. Another exception is the $4f\ ^1F_3$ level, where the effect of mixing on the tensor polarizability is almost 20%; again experiment favors the all mix result. To understand the above results for the tensor polarizability and its relation to the scalar polarizability, we review the theory under some simplifying assumptions.

A. Scalar and tensor polarizabilities in the absence of mixing

1. LS representation

We begin with the theoretical expressions in the simple LS representation. As shown previously [14,20], the single particle scalar and tensor polarizabilities are simply

$$\alpha_{sc}(LS) = -\frac{2L}{3(2L+1)}\left[P(nL, L-1) + \frac{L+1}{L}P(nL, L+1)\right], \tag{11a}$$

$$\alpha_{ten}(LS) = \frac{2L}{3(2L+1)}\left[P(nL, L-1) + \frac{2L-1}{2L+3}P(nL, L+1)\right], \tag{11b}$$

where

$$P(nL, L') = \sum_{n'} \frac{[R_{nL}^{n'L'}]^2}{E_{nL} - E_{n'L'}}. \tag{12}$$

It is understood that the radial matrix elements $R_{nL}^{n'L'}$ and the energies E_{nL} both carry the additional designation of 0 for the singlet and 1 for triplet system. Of course, the above equations can also be derived from Eqs. (5)–(8) by uncoupling L from S, and by setting all mixing angles to zero. As noted previously, the sum in the expression for $P(nL, L')$ is dominated by the term $n' = n$, often contributing close to 99%. Recall from Fig. 2 that some helium $2p$-nd radial matrix elements deviate from the hydrogenic value by as much as 10%. In contrast Fig. 3 shows that the np-nd radial matrix elements are all within 1% of the hydrogenic values for both the singlet and the triplet cases. Needless to say, the helium radial matrix elements for higher L are even closer to the hydrogenic values. Therefore the dipole polarizabilities in helium may be accurately evaluated using the Coulomb approximation, which has been widely used by experimentalists [8,13].

For the circular states where $n = L + 1$, the dominant term in $P(nL, L+1)$ vanishes, and so $P(nL, L+1) \ll P(nL, L-1)$. Comparison of Eqs. (11a) and (11b) shows that then $\alpha_{sc} \simeq -\alpha_{ten}$. In Table V note that this relation generally holds to a few percent for the circular $3d, 4f$, and $5g$ levels in both the singlet and the triplet cases. The somewhat larger discrepancies for the $3d\ ^3D_3$, $4f\ ^1F_3$, and $5g\ ^1G_4$ levels will be discussed in subsection B. Of course, the above equality does not apply to noncircular states, since R_{nL}^{nL+1} does not vanish and in fact $P(nL, L+1)$ is larger than $P(nL, L-1)$. Since E_{nL} is usually ordered

TABLE IV. Tensor polarizabilities in helium [kHz/(V/cm)^2].

Level	No mix	One mix	All mix	Experiment
$3d\ ^1D_2$	-13.98[a]	-13.98[a]	-14.08[a]	-13.9(3)[ab], -14.5(6)[ac]
$3d\ ^3D_3$	2.798[a]	2.798[a]	2.681[a]	2.68(9)[ad]
$4d\ ^1D_2$	-0.4246	-0.4250	-0.4252	-0.421(6)[e], -0.422(3)[f]
$4d\ ^3D_3$	-0.1848	-0.1849	-0.1855	-0.187(3)[d]
$5d\ ^1D_2$	-2.685	-2.687	-2.688	-2.66(6)[e], -2.74(2)[f]
$5d\ ^3D_3$	-1.267	-1.267	-1.269	-1.270(19)[d]
$4f\ ^1F_3$	0.7233	0.6071	0.6064	0.576(9)[g]
$5f\ ^1F_3$	-3.990	-3.999	-4.001	-4.19(12)[g]

[a] In Hz/(V/cm)^2.
[b] Reference [9].
[c] Reference [12].
[d] Reference [10].
[e] Reference [8].
[f] Reference [13].
[g] Reference [11].

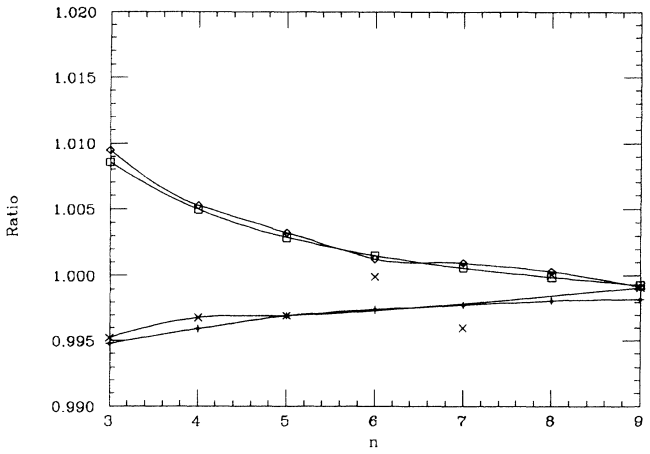

FIG. 3. Ratios of the radial matrix elements $\langle np|r|nd\rangle$ for helium to hydrogen. The same label as in Fig. 2.

in L for the same n, the dominant energy denominator in Eq. (12), $(E_{nL} - E_{nL'})$, usually changes sign from $L' = L - 1$ to $L+1$. In turn this causes the two terms in both Eqs. (11a) and (11b) to have opposite signs.

In summary for a given LS series, the lowest level (the circular state) is expected to have polarizabilities $(\alpha_{sc}, \alpha_{ten})$ of opposite sign and nearly equal magnitudes. For the higher n members of the series, the two types of polarizabilities no longer have nearly equal magnitudes, and will have signs opposite to those of the circular states. These expectations based on the LS representation are well born out in Table V. The only exception is $3d\ ^1D$, where the $3p\ ^1P$ level actually lies above $3d\ ^1D$. The dominant energy denominator $(E_{3d\ ^1D} - E_{3p\ ^1P})$ is therefore negative, unlike all other circular states. Consequently, both polarizabilities of $3d\ ^1D$ have the same signs as all other $nd\ ^1D$ levels.

2. *J*-coupled representation

The relations between the LS- and the J-coupled polarizabilities were first given by Angel and Sandars [14]. We can derive the same relations from Eqs. (5) to (8), assuming all the θ_{nL} vanish. The polarizabilities in the J-coupled representation (without mixing) are related to those in the LS representation by

$$\alpha_{sc}(L\,S\,J) = \alpha_{sc}(LS) \tag{13}$$

and

$$\alpha_{ten}(LSJ) = (-1)^{L+S+J}\left[\frac{J(2J-1)(2J+1)(L+1)(2L+1)(2L+3)}{(J+1)(2J+3)L(2L-1)}\right]^{1/2}\begin{Bmatrix} J & L & S \\ L & J & 2 \end{Bmatrix}\alpha_{ten}(LS). \tag{14}$$

For a two-electron system, they are explicitly

$$\alpha_{ten}(L\,0\,L) = \alpha_{ten}(L0), \tag{15a}$$

$$\alpha_{ten}(L\,1\,L+1) = \alpha_{ten}(L1), \tag{15b}$$

$$\alpha_{ten}(L\,1\,L) = \frac{L^2+L-3}{L(L+1)}\alpha_{ten}(L1), \tag{15c}$$

$$\alpha_{ten}(L\,1\,L-1) = \frac{(L-1)(L+1)(2L-3)(2L+3)}{L^2(2L-1)(2L+1)} \times \alpha_{ten}(L1). \tag{15d}$$

Thus we see that the J-coupled tensor polarizabilities shown in Table IV do indeed correspond to the LS singlet and triplet values. Note that in the absence of mixing, the ratios of the three triplet tensor polarizabilities are fixed. Specific values of the ratios for each L are given in parentheses in the last two columns of Table V. We observe that these ratios are very well satisfied by the D levels, where the mixing angles are small. However, significant departures arise for the F and the G levels, where the mixing angles are large.

TABLE V. Calculated scalar and tensor polarizabilities [kHz/(V/cm)^2] in the "all mix" approximation. Values in ( ) are in LS coupling ( ), and values in [ ] are in the "no mix" approximation.

	α_{sc}		α_{ten}		Ratio to $\alpha_{ten}(LSL+1)$	
Level	^1L_L	$^3L_{L+1}$	^1L_L	$^3L_{L+1}$	^3L_L	$^3L_{L-1}$
					(0.5)	(0.35)
$3d$	14.39[a]	-2.378[a]	-14.08[a]	2.681[a]	0.4987	0.3505
$4d$	1.151	0.7188	-0.4254	-0.1855	0.5006	0.3505
$5d$	7.643	4.813	-2.688	-1.269	0.5005	0.3505
$6d$	31.46	19.74	-10.89	-5.240	0.5005	0.3505
					(0.75)	(0.6857)
$4f$	-0.6529	-0.5293	0.6064[0.722]	0.5308	0.9708	0.6870
$5f$	16.93	17.68	-4.001[-3.99]	-5.304	0.7470	0 6890
$6f$	95.27	98.26	-26.40[-27.0]	-32.50	0.7688	0.6888
$7f$	337.6	347.1	-97.80[-100]	-118.0	0.7723	0.6883
					(0.85)	(0.8185)
$5g$	-16.64	-16.49	15.47	16.49	0.9225	0.8223
$6g$	174.3	169.8	-41.73	-44.64	0.9019	0.8281
$7g$	883.8	873.9	-275.9	-295.0	0.9086	0.8262

[a]In Hz/(V/cm)^2.

Actually, Eqs. (13) to (15) have been derived ignoring the magnetic fine structure splittings in comparison with the electronic energy spacings. For example, for the $3D$ level, the ratio of those energies is 0.3 : 540, and for the $4D$ level it is 0.02 : 7 (all energies in cm^{-1}). Thus this approximation is usually valid to 0.1%. For higher values of L, the fine-structure splitting and the differences in the electronic energy spacings are known analytically [3]. Since the former is proportional to $n^{-3}L^{-2}$ and the latter proportional to $n^{-3}L^{-6}$, we find that the ratio goes as L^{-4}. Specifically, we find that

$$\frac{E_{nL1L-1} - E_{nL1L+1}}{E_{nL+1SJ} - E_{nLSJ}} \simeq \frac{2\alpha^2}{15\alpha_c}(L)(L+1/2)(L+2)(L+5/2), \quad (16)$$

where $\alpha_c = 9/32$ a.u. is the scalar polarizability of He II. Thus for helium, the above ratio is small as long as $L \ll 14$, which is usually the case.

B. Scalar and tensor polarizabilities: effects of mixing

The effect of singlet-triplet mixing on the tensor polarizability has been considered by Aynacioglu *et al.* [11] for the $4f\ ^1F$ and $5f\ ^1F$ levels of helium. They use the Coulomb approximation, and ignore the magnetic fine-structure splittings, both of which we have shown to be valid to within 1%. In addition they invoke a simple scheme of directly mixing the singlet and the triplet polarizabilities. With this procedure, mixing can be expected to alter the value of the polarizabilities since the singlet and the corresponding triplet values may differ by an order of magnitude as well as in sign, as is evident for the $3d$ level in the first 2 rows of Table IV or the first row of Table V. In Appendix A, we deduce from our theory the appropriate expression for the tensor polarizability using the same approximations. The result is somewhat more complicated than their simple expression, involving three mixing angles, not just one. In the case of the F levels where their scheme has been applied, we obtain their result plus an additional term, which contributes 7.5% to α_{ten} in the $4f\ ^1F_3$ sublevel. This point will be elaborated further, as we now elucidate our polarizability results for D, F, and G levels next in turn.

1. Polarizabilities of D levels

We recall that the mixing angles for P and D levels are very small. Hence mixing cannot significantly affect the values of the D polarizabilities, so their results can be easily understood from the viewpoint of the LS representation. In Table IV, the columns "no mix" and "one mix" are nearly equal, well within 0.1% of each other for all D levels. For that matter, there is little difference between columns "one mix" ($n' = n$ only) and "all mix." The greatest difference (4%) resides with the $3d\ ^3D_3$ level. Examination of the composite terms of this tensor polarizability reveals that this difference arises primarily from the contribution of the $4f$ level to the "all mix" value. The $4f\ ^3F$–$3d\ ^3D$ spacing, instead of being typically two orders of magnitude larger because of the change in principal quantum number, is only ten times the $3d\ ^3D$–$3p\ ^3P$ spacing. So for this circular state, the second term in Eq. (11b), $P(3D, F)$, is only one order of magnitude smaller than the first term $P(3D, P)$, and hence, its contribution is not entirely negligible.

Clearly the above discussion on the tensor polarizability also applies to the scalar polarizability. Actually the contribution from the $4f$ level to the $3d\ ^3D_3$ scalar polarizability is considerably larger than that to the tensor polarizability, as the coefficient of the second term, $P(nL, L+1)$, is larger in Eq. (11a) than in Eq. (11b). Since this contribution is opposite in sign to the first term, it reduces the numerical value of the scalar relative to the tensor polarizability by 12%. Table V shows that for the $3d\ ^1D_2$ level, the two polarizability values agree to 2%. Of course, the fact that the same terms in Eqs. (11a) and (11b) dominates the sum, explains why the scalar and the tensor polarizabilities are always opposite in sign for any level. We can also compare the singlet with the triplet value of each polarizability in the same level. For the $3d$ level, they are opposite in sign, unlike all other levels. As noted previously, the $3p\ ^1P$ actually lies above the $3d\ ^1D$ level unlike the $3p\ ^3P$ which lies below the $3d\ ^3D$ level as expected. Therefore the energy denominator of the dominant term in Eq. (12) is opposite in sign for the singlet and for the triplet cases. In fact the ratio of the singlet to the triplet energy denominator is about -1:5, which is in accord with the corresponding ratio of the two polarizabilities shown in Table V. Also displayed in the last two columns are the tensor polarizabilities of the other two sublevels, expressed as ratios to the $J = L + 1$ sublevel in Column 5. Due to the minimal mixing of the D levels, these ratios are practically the same as the theoretical LS coupled ratios shown in parentheses.

For the noncircular nD levels, which begin with n=4, the second term in Eqs. (11a) and (11b) becomes the dominant contributor. In fact using this term alone predicts that the quotient $\alpha_{sc}/\alpha_{ten} = -7/2$ for L=2. From Table V our calculated ratios are -2.7, -2.8, and -2.9 in the ^1D series, and -3.9, -3.8, and -3.8 in the ^3D series, for n=4, 5, and 6, respectively. Further had we kept only the dominant term, with the $(E_{nD} - E_{nF})$ denominator, the singlet and the triplet polarizabilities would be inversely related by the corresponding energy denominator ratios, which turn out to be about 1.4 for all values of $n \geq 4$. The actual ratios of singlet to triplet α_{sc} are 1.6 for all n calculated, and ratios of singlet to triplet α_{ten} are 2.3, 2.1, and 2.1 for n=4, 5, and 6. So it is clear that the first term in Eqs. (11a) and (11b) are far from negligible for the noncircular states. Finally the noncircular tensor polarizabilities for each spin system are plotted on a semilog scale in Fig. 4. Their trend obviously suggests a power law in n, which will be explored in Sec. IV C.

2. Polarizabilities of F levels

Although the mixing angles for F levels are considerable, we still find it convenient to approach their polariz-

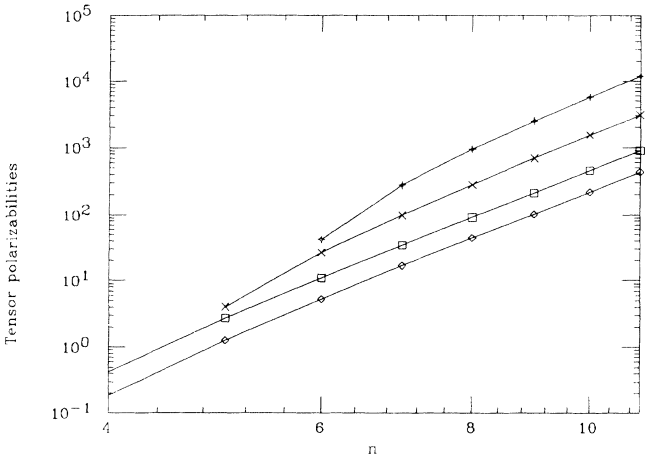

FIG. 4. Tensor polarizabilities in kHz/(V/cm)^2 of noncircular states (absolute value) in a log-log plot against n. The $^3D_3$ values are shown as diamonds, $^1D_2$ as squares, $^1F_3$ as crosses, and $^1G_4$ as bars.

abilities from the simple LS representation. Along with other circular states, the second term in Eqs. (11a) and (11b) is negligible for the $4f$ level, so that $\alpha_{sc}(4F\,S) \simeq -\alpha_{ten}(4F\,S)$ for both S=0 and 1. As in the $3D$ case, we expect the singlet to triplet polarizability ratio to be inversely proportional to the energy denominator $(E_{4F}-E_{4D})$ ratio. Indeed the singlet $\alpha_{ten}(4F\,0)$= 0.7233 under "no mix" in Table IV and the triplet $\alpha_{ten}(4F\,1) \simeq \alpha_{ten}(4f\,^3F_4)$= 0.5308 in Column 5 of Table V reflect the above energy ratio. However, when mixing is taken into account in "one mix" of Table IV, the singlet $4F$ value decreases by some 20% to 0.6071. As shown in Appendix A, the treatment of Aynacioglu *et al.* [11] in mixing $\alpha_{ten}(4F\,0)$ and $\alpha_{ten}(4F\,1)$ is not consistent with theory. Indeed, the difference between theirs and our result is given by Eq. (A7), which is about 8% for the $4f$ level. Comparison with their calculated value of 0.601 for $\alpha_{ten}(4F\,0)$ is complicated by their using $\theta_{4F} = 41.8°$ rather than our value of 37.1°, which is consistent with their later measurement [21] . In fact, the next column "all mix", including many terms in the sum of Eq. (12), gives essentially the same result. Unfortunately, this value is still more than three standard deviations from experiment. Our analysis leaves no room for theoretical errors, and indeed in all other cases, Table IV shows that our theory agrees closely with experiment . Thus we can only attribute the discrepancy in the $4f\,^1F_3$ α_{ten} to experimental errors, e.g., the deconvolution with the signal from the $4f\,^3F_3$ sublevel may be incomplete. Similarly, mixing also affects the scalar polarizability for the $4f\,^1F_3$ sublevel changing its value from −0.7209 to −0.6529.

On the other hand, neither of the polarizabilities of the $4f\,^3F_4$ sublevel is significantly affected by mixing. Table V shows that $\alpha_{sc}(4f\,^3F_4)$= −0.5293 and $\alpha_{ten}(4f\,^3F_4)$=0.5309 (which are identical to the no mix results). As anticipated, they are opposite in sign and essentially equal numerically. Similar results are obtained for the $4f\,^3F_2$ sublevel, whose ratio of α_{ten} to that of the $4f\,^3F_4$ sublevel is virtually the same as the LS value of 0.6857 in Column 7. However, unlike the other two sublevels, the $4f\,^3F_3$ sublevel is strongly mixed with the $4f\,^1F_3$, thereby increasing its α_{ten}, and hence its ratio in Column 6 is substantially larger than the LS value of 0.75.

The rest of the nF levels are noncircular, and so behave analogously to the noncircular nD levels. Accounting only for the dominant second term in Eqs. (11a) and (11b) implies the quotient α_{sc}/α_{ten}= −12/5 in both the singlet and in the triplet system. Examination of Table V reveals that the values of these ratios are substantially different, typically −3 to −4. As L increases, the energy denominators in Eq. (12) are accurately given by the polarization formula (see Ref. [3]), and so the first term becomes more comparable to the second. As a matter of fact, the polarization formula does not distinguish between the singlet and the triplet systems, and we observe that the singlet and triplet values for α_{sc} are indeed within a few percent of each other for n=5, 6, and 7. However values for the α_{ten} are further apart, reflecting the greater role played by the first term in Eq. (11b). As we recall, the smaller singlet denominator $(E_{nD} - E_{nF})$ enhances its partial cancellation with the second term, and thus reducing the numerical value of the singlet more than the triplet α_{ten}.

Unlike the $4f\,^1F_3$ case where mixing changes α_{ten} by 20%, Table IV shows that mixing affects the $5f\,^1F_3$ value by less than 1%. Similarly, Table V shows that mixing has a small effect on the triplet $5F$ sublevels, since the ratios agree well with the LS-coupling values. So how can mixing be important for the $4F$ but unimportant for F levels with $n \geq 5$, when Fig. 1 shows that θ_{nF} depends only mildly on n? The answer is provided in Eq. (A8) in Appendix A, which shows that the mixed and the unmixed polarizabilities differ by

$$\sin^2\theta_{nF}\,[(3/4)\alpha_{ten}(F1) - \alpha_{ten}(F0)]\,. \qquad (17)$$

The unmixed polarizabilities in the LS representation for the F levels may be obtained from Table V, using $\alpha_{ten}(^3L_{L+1})$ for the unmixed triplet, and the quantities in brackets for the unmixed singlet. It can be seen that the quantity in the square brackets in Eq. (17) coincidentally almost vanishes for the $5F$ level. For higher nF levels, the square bracket remains small but not negligibly so, and mixing affects these values by a few percent.

3. *Polarizabilities of G levels*

As far as we know, there has been no measurement of the polarizabilities of any G level. Table V shows our calculated values for the $5G$, $6G$, and $7G$ levels. As expected, the singlet and the triplet values are rather similar especially for α_{sc}. For the circular $5G$ level, the anticipated $\alpha_{sc} \simeq -\alpha_{ten}$ is very well satisfied in the triplet but not so well in the singlet case. Column 6 shows that in the LS representation, the α_{ten} ratio for the $^3G_4$ sublevel is 0.85. Hence mixing reduces the numerical value of the $^1G_4$ sublevel while it increases that of the $^3G_4$ sublevel, causing the triplet α_{ten} ratio to rise significantly above the LS value in parentheses. The above discussions apply to the noncircular nG levels, except for the

near equality of the two polarizabilities. Here the ratios of those two polarizabilities are more like -4 rather than $\alpha_{sc}/\alpha_{ten} = -55/28$ as Eqs. (11a) and (11b) would suggest, assuming the second term dominates in both. We will see what the trends are and how to evaluate the polarizabilities of higher L levels in the next subsection.

C. Analytic fits and trends in the polarizabilities

We have just seen that the polarizabilities in the mixed J-coupled representation can always be approximately expressed in terms of those in the LS representation. Further, we recall that the relevant matrix elements (those with $n' = n$) are accurately given by the hydrogenic expressions. With the supposition of an n-independent quantum defect μ_L , we find that

$$\alpha_{ten}(nLS) = -C_L n^2 (n-\mu_L)^2 \times\left[\frac{(2L-1)[n^2-(L+1)^2](n-\mu_{L+1})^2}{\mu_d^+(n-\mu_a^+)} - \frac{(2L+3)(n^2-L^2)(n-\mu_{L-1})^2}{\mu_d^-(n-\mu_a^-)}\right], \quad (18)$$

where $C_L = 3L/[2(2L+1)(2L+3)]$, and $\mu_d^- = \mu_{L-1} - \mu_L$, $\mu_d^+ = \mu_L - \mu_{L+1}$, and $\mu_a^\pm = (\mu_{L\pm1} + \mu_L)/2$.

1. Circular states

For circular states ($n = L+1$), we observe that the first term in Eq. (18) vanishes, which leads to the now familiar result $\alpha_{sc} \simeq -\alpha_{ten}$. Further, for sufficiently high L (≥ 3 for helium), the quantum defect is well approximated by the polarization formula,

$$\mu_L \simeq \alpha_c \frac{3n^2 - L(L+1)}{4n^2(L-1/2)L(L+1/2)(L+1)(L+3/2)}, \quad (19)$$

where α_c=9/32 (in a_0^3) is the scalar polarizability of the helium core. With these considerations, we find

$$\alpha_{ten}(L) = (L-3/2)(L-1)(L-1/2) \times L(L+1/2)n^7/(2\alpha_c), \quad (n = L+1). \quad (20)$$

Thus we see that α_{ten} (and also α_{sc}) is inversely proportional to the core polarizability α_c, and it varies as n^7 as will be demonstrated for noncircular states, where n and L are independent.

2. Noncircular states

If in Eq. (18) we take all $\mu \ll n$, we can rewrite it as a series in decreasing powers of n where the leading term is n^7. In Appendix B, we give the first few coefficients for both α_{ten} and α_{sc}. It is interesting to observe that both coefficients of n^6 depend on the ratios μ_a/μ_d while the other coefficients depend on the inverse of μ_d. When L is sufficiently high so that the quantum defects are small, the former becomes negligible. Even for L as low as 2, we find that the coefficients of n^6 are three orders of magnitudes less than those of n^7. Thus it is sufficient to include just the odd power terms in the series, and in fact we found that only two terms are necessary to represent the polarizabilities to an accuracy of a few percent. The coefficients for α_{ten} are given in Table VI for the $n\,{}^1D_2$, $n\,{}^3D_3$, $n\,{}^1F_3$, and the $ng\,{}^1G_4$ series. When L is sufficiently large ($L \geq 4$), we find

TABLE VI. Power-law coefficients for α_{ten} [in kHz/(V/cm)^2].

Series	T_7	T_5
$^3D_3$	-2.38×10^{-5}	1.66×10^{-4}
^1D	-4.89×10^{-5}	3.41×10^{-4}
^1F	-1.64×10^{-4}	2.66×10^{-3}
^1G	-7.75×10^{-4}	1.94×10^{-2}

$$T_7 = -2.49\times10^{-8}L(L-1/2) \times(8L^3+12L^2-5L-9/2)/\alpha_c, \quad (21a)$$

$$T_5 = 4.98\times10^{-9}(L-1/2)L(L+1/2) \times(48L^4+96L^3+16L^2-32L-9)/\alpha_c. \quad (21b)$$

For example, Eq. (21a) yields a value of $T_7 = -8.42 \times10^{-4}$ for L=4. Then Eq. (A4) implies that the leading coefficient of $\alpha_{ten}(^1G_4)$=-7.70×10^{-4}, which is in good agreement with the value -7.75×10^{-4} in Table VI. Thus we see that the polarizabilities are proportional to L^5n^7/α_c in the high n and L limits .

However, it should be emphasized that the above formulas for both circular and noncircular states are valid for high L as long as $L \ll 14$ for helium. (See Sec. IV A 2.) For example, the error is estimated to be about $2^{-4} \simeq 6$ % for L=7. Thus for $L \geq 8$, it is probably advisable to return to Eqs. (5) to (8), and explicitly account for the fine structure. Finally for sufficiently high values of L, n, and $\mathcal{E}$, nondegenerate perturbation theory fails, and one must diagonalize the full Hamiltonian. Indeed, the Stark effect becomes linear in the extreme limit.

V. CONCLUSIONS

We have calculated the radiative lifetimes and the scalar and tensor polarizabilities of excited levels of helium. Our computation is the most complete to date in that it utilizes the best available dipole matrix elements, transitions to all fine-structure sublevels, and the mixing of singlet and triplet levels. The results are in excellent agreement with experiment, with the exception of the $\alpha_{ten}(4f\ ^1F)$, where the discrepancy is three standard deviations and a plausible explanation is offered. However, it should also be said that the present results have not changed significantly from previous simpler theories. What we have gained are insights as to why the additional effects are generally unimportant, except for mixing in the calculation of polarizabilities when $L \geq 3$. In addition, we have found approximate relations between various polarizabilities considered here, and given predictions of their values at higher n and L.

Since electronic correlation in an excited helium atom

is weak, the matrix elements in Theodosiou's model potential usually come within 1% of the accurate results of Kono and Hattori. (The largest discrepancy of 1.5% resides in the $2S$-$3P$ triplet matrix element, thereby reducing Theodosiou's lifetime for the $3p\ ^3P$ level from [7] 98.15 to 94.82 ns.) For the polarizabilities, which depend primarily on the matrix elements of the resonance transition, even the simple hydrogenic approximation is shown to be adequate. The magnetic fine-structure splitting is seen to be unimportant as it is typically three orders of magnitude lower than the electronic energy. For $L \leq 2$, mixing is unimportant because the mixing angles are too small. For F levels, we confirm the importance of mixing as discussed by Aynacioglu *et al.* However, their scheme to account for mixing is shown to be inadequate. We have derived the corresponding expression from first principles, using the same approximations. The result is their expression plus an additional term, which in the $4f\ ^1F_3$ case contributes 7.5%. Further we give expressions for easy calculation of lifetimes and polarizabilities for higher n and L values.

Finally, we discuss what our findings in helium portends for other atoms. For high values of L ($L \geq 4$ for elements up to copper), most of this work is applicable. We must of course use the appropriate core polarizability, which is usually much larger than in helium, e.g., its value is two orders of magnitude larger in magnesium [22]. When the core is not in a S state, electric quadrupole interactions further complicate the level structure and the polarizabilities, and have been dealt with in neon [23] and in iron [24], disregarding mixing. For some of these cases, mixing can now be included, following the semiempirical approach of Curtis [25].

ACKNOWLEDGMENTS

We thank Professor G. von Oppen for useful communications in the early stages of this work.

APPENDIX A: SIMPLIFIED SINGLET TENSOR POLARIZABILITIES WITH MIXING

From Eqs. (5) to (8), we now make the approximations that the magnetic fine structure is negligibly small and that only the resonance terms ($n' = n$) need to be included. Under these circumstances, it is possible to express the polarizabilities in the mixed J-coupled representation in terms of the simple LS-coupled ones. We focus on the singlet tensor polarizability, where measurements are more abundant. Adopting the shorthand notation c_L=cos θ_{nL} and s_L=sin θ_{nL} for the singlet and triplet component amplitudes, we specifically find

$$\begin{aligned}\alpha_{\rm ten}(nL0L) = \frac{2L}{3(2L+1)(2L+3)}\Bigg[&\left(1-\frac{3}{L(L+1)}s_L^2\right)\left(\frac{(2L+3)[R_{nL}^{nL-1}]^2}{E_{nL,0}-E_{nL-1,0}}-\frac{(2L-1)[R_{nL}^{nL+1}]^2}{E_{nL+1,0}-E_{nL,0}}\right)\\ &+(f_{01}^{L,L-1}-1)\frac{(2L+3)[R_{nL}^{nL-1}]^2}{E_{nL,0}-E_{nL-1,0}}\left([-c_Ls_{L-1}+s_Lc_{L-1}\sqrt{1-L^{-2}}]^2-\frac{(2L-1)}{L^2(L+1)}s_L^2\right)\\ &-(f_{10}^{L+1,L}-1)\frac{(2L-1)[R_{nL}^{nL+1}]^2}{E_{nL+1,0}-E_{nL,0}}\left([-c_Ls_{L+1}+s_Lc_{L+1}\sqrt{1-(L+1)^{-2}}]^2-\frac{(2L+3)}{L(L+1)^2}s_L^2\right)\Bigg],\end{aligned} \tag{A1}$$

where

$$f_{01}^{L,L-1}=\frac{E_{nL,0}-E_{nL-1,0}}{E_{nL,0}-E_{nL-1,1}},$$
$$f_{10}^{L+1,L}=\frac{E_{nL+1,0}-E_{nL,0}}{E_{nL+1,1}-E_{nL,0}}.$$

When L is sufficiently low so that all three mixing angles (θ_{L-1}, θ_L, and θ_{L+1}) are negligibly small, we recover the LS result given by Eq. (11b), with the singlet energy denominators.

For L=2, Fig. 1 shows that the first two angles are negligibly small, but not the third, $\theta_{nF} \simeq 30°$. Neglecting those two angles reduces Eq. (A1) to

$$\alpha_{\rm ten}(nd\ ^1D_2)=\frac{4}{105}\left[7\frac{[R_{nD}^{nP}]^2}{E_{nD,0}-E_{nP,0}}-3\frac{[R_{nD}^{nF}]^2}{E_{nF,0}-E_{nD,0}}\times[1+\sin^2\theta_{nF}(1-f_{10}^{F,D})]\right]. \tag{A2}$$

We recognize that the first two terms simply give the singlet LS-coupled $\alpha_{\rm ten}(nD0)$. In the last term,

$$f_{10}^{F,D}=\frac{E_{nF,0}-E_{nD,0}}{E_{nF,1}-E_{nD,0}}, \tag{A3}$$

has a typical value of 1.004. Thus, the third term yields a negligible contribution, which is only 0.1% of the second term. So we have demonstrated that mixing does not affect $\alpha_{\rm ten}$ for D levels significantly.

For L=3, the situation is quite different since we have only one negligible angle, θ_{nD} with the other two angles being large. Further, the G levels (and to a lesser extent the F levels) are nearly degenerate so that $E_{nG,0} \simeq E_{nG,1} \simeq E_{nG}$, and hence the last line of Eq. (A1) vanishes. Under these circumstances, we find

$$\begin{aligned}\alpha_{\rm ten}(nf\ ^1F_3)=\frac{2}{63}\Bigg[&\frac{9[R_{nF}^{nD}]^2}{E_{nF,0}-E_{nD,0}}\times\left(\cos^2\theta_{nF}+\frac{3}{4}\sin^2\theta_{nF}f_{01}^{F,D}\right)\\ &-\frac{5[R_{nF}^{nG}]^2}{E_{nG}-E_{nF,0}}\left(1-\frac{1}{4}\sin^2\theta_{nF}\right)\Bigg],\end{aligned} \tag{A4}$$

where

$$f_{01}^{F,D} = \frac{E_{nF,0} - E_{nD,0}}{E_{nF,0} - E_{nD,1}}. \quad \text{(A5)}$$

Our derived approximate equation resembles, but is not the same as the expression postulated by Aynacioglu *et al.* [11]. Since the exchange energy of the F levels is neglectable in comparison to the $nD - nF$ spacing, we may recast their expression in our notation as

$$\alpha_{\rm ten}^{\rm Aynac}(nf\ ^1F_3) = \frac{2}{63}\left[\frac{9[R_{nF}^{nD}]^2}{E_{nF,0} - E_{nD,0}} \times(\cos^2\theta_{nF} + \sin^2\theta_{nF} f_{01}^{F,D}) - \frac{5[R_{nF}^{nG}]^2}{E_{nG} - E_{nF,0}}\right]. \quad \text{(A6)}$$

In fact we find that the two differ by

$$\text{Eq. (A6)} - \text{Eq. (A4)} = (\sin^2\theta_{nF}/4)\alpha_{\rm ten}(nf\ ^3F_4). \quad \text{(A7)}$$

Alternatively, we can express the mixed J-coupled tensor polarizability Eq. (A4) in terms of the unmixed LS quantity Eq. (11b),

$$\alpha_{\rm ten}(nf\ ^1F_3) = \alpha_{\rm ten}(F0) + \sin^2\theta_{nF} \times[(3/4)\alpha_{\rm ten}(F1) - \alpha_{\rm ten}(F0)]. \quad \text{(A8)}$$

For L=4 and higher values, the distinction between singlet and triplet energies vanishes. Thus the last two lines in Eq. (A1) become negligible, and we obtain the simple result

$$\alpha_{\rm ten}(n\,^1L_L) = \left[1 - \frac{3}{L(L+1)}\sin^2\theta_{nL}\right]\alpha_{\rm ten}(nL). \quad \text{(A9)}$$

Since $\theta_{nL} = \pi/2 - [6(2L+1)]^{-1} \simeq 45°$, the bracket in Eq. (A9) is approximately $\{1 - 3[2L(L+1)]^{-1}\}$. Thus the singlet tensor polarizability is smaller than the corresponding LS value by 7.5% for G, and 5% for H levels. Simultaneously, $\alpha_{\rm ten}(n\,^3L_3)$ increases by the same amount.

APPENDIX B: ANALYTIC COEFFICIENTS FOR POLARIZABILITY POWER SERIES

In Eq. (18) if we collect equal powers of n, we find that it forms a descending series where the leading term is $T_7\,n^7$. Explicitly, the first few coefficients are

$$T_7 = -C_L\left[\frac{2L-1}{\mu_d^+} - \frac{2L+3}{\mu_d^-}\right], \quad \text{(B1a)}$$

$$T_6 = 4C_L\left[(2L-1)\frac{\mu_a^+}{\mu_d^+} - (2L+3)\frac{\mu_a^-}{\mu_d^-}\right], \quad \text{(B1b)}$$

$$T_5 = C_L\left[\frac{2L-1}{\mu_d^+}B^+ - \frac{2L+3}{\mu_d^-}B^-\right], \quad \text{(B1c)}$$

$$\vdots$$

where $B^+ = [(L+1)^2 - 4(\mu_a^+)^2 - 2\mu_L\mu_{L+1}]$ and $B^- = [L^2 - 4(\mu_a^-)^2 - 2\mu_{L-1}\mu_L]$. Similarly, the coefficients for the scalar polarizability are found to be

$$S_7 = D_L\left[\frac{L+1}{\mu_d^+} - \frac{L}{\mu_d^-}\right], \quad \text{(B2a)}$$

$$S_6 = -4D_L\left[(L+1)\frac{\mu_a^+}{\mu_d^+} - L\frac{\mu_a^-}{\mu_d^-}\right], \quad \text{(B2b)}$$

$$S_5 = -D_L\left[\frac{L+1}{\mu_d^+}B^+ - \frac{L}{\mu_d^-}B_-\right], \quad \text{(B2c)}$$

$$\vdots$$

where $D_L = 3/[2(2L+1)]$.

It is interesting to observe that both coefficients of n^6 depend on the ratios μ_a/μ_d while the other coefficients depend on the inverse of μ_d. For nonpenetrating states where the quantum defects are small, the former becomes negligible. Then the series has only the odd-power terms, as found for D and higher L levels of helium. On the other hand for penetrating states, the quantum defects can be comparable to n, so the coefficients of n^6 may be sizable, as found for the D series of rubidium [26].

[1] A. Kono and S. Hattori, Phys. Rev. A **29**, 2981 (1984).
[2] A. Kono and S. Hattori, Phys. Rev. A **31**, 1199 (1985).
[3] E.S. Chang, Phys. Rev. A **35**, 2777 (1987).
[4] C.E. Theodosiou, Phys. Rev. A **30**, 2910 (1984).
[5] E.S. Chang, Phys. Rev. A **31**, 495 (1985).
[6] H. Marxer and L. Spruch, Phys. Rev. **A 43**, 1268 (1991).
[7] C.E. Theodosiou, At. Data Nucl. Data Tables, **36**, 97 (1987).
[8] D. Szostak, G. von Oppen, and W.-D. Perschmann, Phys. Lett. A **76**, 376 (1980).
[9] G. v. Oppen, W. Schilling, and Y. Kriescher, Z. Phys. A, **321**, 91 (1985).
[10] W.-D. Pershmann, G. von Oppen, and D. Szostak, Z. Phys. A **311**, 49 (1983).
[11] A.S. Aynacioglu, G. v. Oppen, W.-D. Perschmann, and D. Szostak, Z. Phys. A **303**, 97 (1981).
[12] Y. Ouerdane, A. Dennis, and J. Desesquelles, Phys. Rev. A **34**, 1966 (1983).
[13] A. Denis, Y. Ouerdane, G. Docao, and J. Desequelles, J. Physiques **48**, 227 (1987).
[14] J.R.P. Angel and P.G.H. Sandars, Proc. R. Soc. London, Sect. A **305**, 125 (1968).
[15] Ya. Verolainen and A. Ya. Nikolaich, Usp. Fiz. Nauk. **137**, 305 (1982) [Sov. Phys. Usp. **25**, 431 (1982)].
[16] W.C. Martin, Phys. Rev. A **36**, 3575 (1987); J.S. Sims and W.C. Martin, *ibid.* **37**, 2259 (1988).
[17] N. Bessis, G. Bessis, and G. Hadinger, Phys. Rev. A **8**, 2246 (1973).
[18] S. Hameed, A. Herzenberg, and M.G. James, J. Phys. B **1**, 822 (1968).
[19] A. Wolf, G. v. Oppen, W.-D. Perschmann, and D. Szostak, Z. Phys. A **292**, 319 (1979).
[20] E.S. Chang and W.G. Schoenfeld, Astrophys. J. **383**, 450 (1991); Note missing brackets and typographical error in Eq. (A3).
[21] W. Schilling, Y. Kriescher, A.S. Aynacioglu, and G. v.

Oppen, Phys. Rev. Lett. **59**, 876 (1987).
[22] E.S. Chang, Phys. Scr. **35**, 792 (1987).
[23] E.S. Chang, W.G. Schoenfeld, E. Biémont, P. Quinet, and P. Palmeri, Phys. Scr. **49**, 26 (1994).
[24] E.S. Chang, W.G. Schoenfeld, M. Geller, S. Johansson, G. Nave, A.J. Sauval, and N. Grevesse (unpublished).
[25] L.J. Curtis, Phys. Rev. A **40**, 6958 (1989).
[26] M.S. O'Sullivan and B.P. Stoicheff, Phys. Rev. A **33**, 1640 (1986).